Photolysis of the Herbicide Dicamba in Aqueous Solutions and on Corn (Zea Maize) Epicuticular Waxes

SCHOLARONE™
Manuscripts

1
2
3
4

Photolysis of the Herbicide Dicamba in Aqueous Solutions and on Corn (*Zea Maize*) Epicuticular Waxes

3

4   Kaitlyn Gruber

5   Brittany Courteau[+]

6   Maheemah Bokhoree

7   Elijah McMahon

8   Jenna Kotz

9   Amanda Nienow*

10

11

12   Gustavus Adolphus College

13   800 W College Avenue

14   St. Peter, Minnesota 56082, United States

15
16

17   January 21, 2021

19
20
21
22
23
24
25

26 [+] Present Address: Department of Chemistry, Iowa State University, 1605 Gilman Hall, Ames,
27 IA 50011
28 *Author to whom correspondence should be addressed: Telephone: (507) 933-7327, fax: (507)
29 933-7041, Email: anienow@gustavus.edu.
30

1
2
3
4
5
6
7
8
9
10
11
12
13
14
15
16
17
18
19
20
21
22
23
24
25
26
27
28
29
30
31
32
33
34
35
36
37
38
39
40
41
42
43
44
45
46
47
48
49
50
51
52
53
54
55
56
57
58
59
60

31   Abstract

32   Dicamba, 3,6-Dichloro-2-methoxybenzoic acid, has been used in agriculture as an herbicide for

33   over fifty years, and has seen an increase in use in the past decade due to the development of

34   glyphosate resistant weeds and soybeans genetically modified to resist dicamba. Despite the

35   previous use of dicamba, many questions remain regarding its environmental fate, especially the

36   new commercial formulations used on genetically modified crops. Here, the photolysis of

37   dicamba, including the commercial formulation Diablo®, is examined in aqueous solutions of

38   varying water quality and on the surface of corn epicuticular waxes. Dicamba is stable to

39   hydrolysis but degrades under UV light. The photolytic half-life for dicamba photolysis in

40   aqueous solutions at pH 7 irradiated with Rayonet UVB lamps (280-340 nm) was $t_{1/2}$ = 43.3 min

41   (0.72 hours), in aqueous solutions at pH 7 in a Q-Sun solar simulator (λ > 300 nm) was $t_{1/2}$ =

42   13.4 hours, and on epicuticular waxes irradiated in the Q-sun solar simulator was $t_{1/2}$ = 105

43   hours. Experiments with adjuvants, compounds added into the commercial formulations of

44   dicamba, led to increases in rate constants for both aqueous and wax experiments. In addition to

45   kinetic rate constants, photoproducts were tentatively assigned for the aqueous solution

46   experiments. This work deepens the knowledge of the environmental fate of dicamba including

47   the role surfactants play in chemical reactions and in providing new applications of current

48   methods to examine the photolysis of chemicals sorbed to surfaces.

49

50   Environmental Significance Statement

51   In 2016, Monsanto announced Roundup Ready 2 soybeans, genetically modified soybeans that

52   can tolerate dicamba and glyphosate. With the increased use of dicamba on soybeans, a crop to

53   which it has not been previously applied, it has become apparent that herbicide drifting causes

54   crop damage in adjacent fields; thus, understanding the environmental fate of dicamba is

55   essential for maintaining ecological health. This project provides details on the environmental

56   fate of dicamba by examining its photochemical reactivity when sorbed to epicuticular waxes, in

57   the presence of adjuvants, and in commercial formulation. The methods used in this work can be

58   extended to examine the photolysis of other pesticides and new pesticide formulations.

59 INTRODUCTION

60 Agrochemicals are widely used around the world. In 2012, 1,182 million pounds of pesticides

61 were used in agriculture in the United States; 678 million pounds of that amount was herbicides

62 dedicated to the eradication of weeds.[1] For over 50 years, dicamba, 3,6-Dichloro-2-

63 methoxybenzoic acid, has been one of the agrochemicals used in the United States, historically

64 mostly on corn or grain crops. With a pKa of 1.87 or 1.94,[2] dicamba is a weak acid that causes

65 death in most plants by targeting the plants' vascular tissue. Past formulations of dicamba have

66 been listed as a restricted-use herbicide due to high potential to volatilize, leach from soils,

67 persist in groundwater, and to cause widespread contamination of ecosystems.[3–10] The use of

68 dicamba decreased upon the rise of glyphosate in the early 2000s, but the recent development of

69 glyphosate resistant weeds means dicamba use is increasing again (as seen by USDA data

70 analyzed on the Pesticide Use Data System of Hygeia Analytics).[11,12] In 2016, Monsanto

71 announced Roundup Ready 2 soybeans, genetically modified soybeans branded under the name

72 Xtend, that can tolerate both dicamba and glyphosate.[13] In April 2016, the EPA allowed the use

73 of dicamba in sprays for these soybeans for five years.[14] In July 2016, the Xtend soybeans gained

74 EU import approval.[15] Despite conditional approval and restrictions on use, growing season 2017

75 saw the first use of Xtend soybeans in the US - and by the end of the summer, there were

76 thousands of complaints from farmers with fields adjacent to those using Xtend soybeans. It has

77 since been shown in the scientific literature that dicamba drifting is a probable cause for the crop

78 damage in adjacent fields.[16] After lawsuits by several environmental groups, a federal circuit

79 court revoked the EPA approval to use dicamba in June 2020; a week later, the EPA banned the

80 sale of specific dicamba products but said farmers can spray any dicamba products already in

81 their possession.[17] 2020 already marked the end of federal approval of dicamba products, and

82 manufacturers would already have been submitting new applications for approval for use of the

83 products in 2021.[18] In addition, these rulings only impact the newest formulations of dicamba

84 product. Although the future of dicamba use in agriculture is uncertain, it is imperative to

85 examine the chemistry of the molecule to better understand the environmental fate of the

86 product.

87

88 Biodegradation, photodegradation, and chemical reactions are the three main pathways for

89 eliminating pollutants from the environment. In the literature, dicamba is observed to be stable in

90 aqueous conditions and does not undergo hydrolysis as a degradation pathway.[2] The

91 biodegradation of dicamba has been examined in many publications.[19–22] There are a handful of

92 papers in the literature exploring the photochemistry of dicamba, but most of the previous work

93 on the photochemistry of dicamba has been done in aqueous solutions with advanced oxidation

94 processes (AOP) such as the use of UV/H_2O_2 to degrade the molecule,[4] on photocatalysis

95 processes such as using TiO_2 as a catalyst,[4,23,24] or the photo-Fenton reaction[2,25] to degrade the

96 molecule. There has been no work investigating the photochemistry of formulated dicamba on

97 the surface of crops or examining the role adjuvants, like those added in commercial

98 formulations, have on the photochemistry of dicamba. Here we examine the photochemistry of

99 dicamba in aqueous solution (without advanced oxidation processes), in solution with a model

100 adjuvant, and on the surfaces of epicuticular waxes collected from corn plants. The

101 photochemistry of the commercial product Diablo® was also examined in aqueous solution and

102 on the epicuticular waxes.

103

104 MATERIALS AND METHODS

105 Chemicals and Instrumentation

106 Analytical standards of dicamba (Sigma-Aldrich, >98.9%) were produced ranging from 0.2 mg/L

107 to 40 mg/L in Milli-Q water (Milli-Pore). The commercial formulation of dicamba, Diablo®, was

108 acquired from Red River Specialties, LLC and used as received. Diablo® was diluted from 480

109 g/L to 15 mg/L in 1 mM pH 7 phosphate buffer. Chromatographic solvents, such as acetonitrile

110 (ACN, ≥99.9%) and water (>99.9% HPLC-grade), were purchased from Sigma-Aldrich.

111 Phosphate buffers were prepared using H_3PO_4, $NaH_2PO_4 \cdot H_2O$, or $NaHPO_4 \cdot 3H_2O$ (Fisher

112 Scientific) as needed in Milli-Q water and were 1 mM in total phosphate. Natural organic matter

113 (NOM) was obtained from the International Humic Substance Society (IHSS) collected from the

114 Suwannee River (1R101N). Actinometry solvents used were methanol (Sigma-Aldrich, ≥99.9%

115 or EM Science, 99.97%), p-nitroacetophenone (Aldrich, 98%), and pyridine (Sigma-Aldrich,

116 99.8%). The adjuvant MAKON® DA-6 was obtained as a sample from the Stepan Company of

117 Northfield, IL. MAKON® DA-6 is a non-ionic surfactant containing mostly isodecyl alcohol

118 ethoxylate.

119

120 HPLC analysis for dicamba was performed using 1290 Infinity autosampler and binary pump,

121 1200 series thermostatted column compartment and 1100 series diode array detector (Agilent)

122   and a reversed-phase 50 mm × 2.1 mm i.d. Eclipse Plus C18, 1.8b micron, S/N: USDAY 40893

123   column (Agilent). The mobile phase consisted of aqueous %A 1.7 mF phosphate buffer (pH ~3)

124   and %B ACN in a gradient of 20-50-75-20-20 %B at 0-3.5-4.0-4.01-5 minutes. A flow rate of

125   0.5 mL/minutes and a run time of 5 minutes were used. Sample injection volume was 20 μL,

126   column temperature 36°C, and UV-Vis detection set at 220 and 254 nm wavelengths.

127   Chromatographic results from HPLC analysis for dicamba are displayed at 220 nm.

128

129   The p-nitroacetophenone/pyridine samples from the quantum yield experiments were analyzed in

130   the HPLC using the same instrumentation and mobile phase. A reversed-phase 75 x 2.1 mm i.d.

131   ACE Excel 3 Super C18, S/N: A116046 column (Advanced Chromatography Technologies

132   LTD) was used with a gradient of 2-80-80-2-2 %B at 0-0.75-1.0-1.01-1.25 minutes. A flow rate

133   of 0.6 mL/min was used with a stop time of 1.25 minutes, 1 μL sample injection volume, and a

134   column temperature of 50°C. UV-Vis detection was monitored at 288, 254, and 220 nm

135   wavelengths. Chromatographic results from the HPLC analysis for p-nitroacetophenone/pyridine

136   are displayed at 288 nm.

137

138   Photolysis of Dicamba in Aqueous Solutions

139   The photolysis of dicamba was examined with three different irradiation sources: a Q-Sun Xe-1

140   Solar Simulator with a Daylight-Q filter, a Rayonet RPR-100 Photochemical Reactor (Southern

141   New England Ultraviolet Company), and outdoors in St. Peter, MN on the Gustavus Adolphus

142   College campus (44° 20' 0" N, 93° 58' 0" W) in June 2019.

143

144   The photolysis of dicamba in aqueous solution (15 mg/L) with the Q-Sun Xe-1 Solar Simulator

145   was with a Xe lamp, an irradiance of 0.40 W m^2 at 340 nm, a nominal cut-on of 295 nm, and at

146   30 °C. The spectral irradiance of the lamp is shown in Figure S-21 along with the UV-Vis

147   absorbance spectra of dicamba. Each sample of dicamba was prepared by dissolving the

148   necessary amount of solid in phosphate buffer (at pH 7), followed by sonication for 20 minutes.

149   10 mL of the 15 mg/L dicamba solution was added to two glass petri dishes which were then

150   placed into the Q-Sun solar simulator for irradiation. Simultaneously, two petri dishes containing

151   PNAP/PYR actinometer were also irradiated (see details on actinometry below). Every two

152   hours, samples were collected from the four petri dishes: solvent was first added back to the petri

153   dishes until the dishes contained 10 mL again (to account for evaporation), then 100 µL of

154   sample was collected into HPLC vials with glass inserts and set aside for HPLC analysis.

155   Samples were collected every two hours over four 8-hour periods with samples being stored in

156   the refrigerator at 9 °C between the four periods.

157

158   Multiple photochemical aqueous solution reactions of dicamba (15 mg/L) were conducted using

159   a 600 mL quartz reaction flask filled with ~500 mL dicamba, held in a Rayonet RPR-100

160   Photochemical Reactor (Southern New England Ultraviolet Company). Each sample of dicamba

161   was prepared by dissolving the necessary amount of solid in desired solvent, usually phosphate

162   buffer (at pH 7), HCl solution (pH 1), or Milli-Q water, followed by sonication for 20 minutes.

163   In experiments with additions of adjuvant or NOM, the appropriate compound (0.24 mL of a

164   1.05% (w/w) MAKON® DA-6 stock to make 5 mg/L DA-6 or solid NOM to make solutions of 1

165   mg/L, 5 mg/L, or 10 mg/L) was added after sonication. For quenching reactions, isopropanol

166   (final concentration of 1%) or l-histidine (final concentration of 5 mM) was added to the solution

167   immediately prior to irradiation. In the experiment conducted with H_2O_2, 283 µL of 30% H_2O_2

168   was added after sonication of the 15 mg/L dicamba solution. For the experiments using

169   Minnesota River water, river water was collected using new sample bottles that were rinsed three

170   times before collection and then river water was filtered using a Millipore glass vacuum filter

171   with fiber glass filter paper (5 microns). Dicamba was added to the filtered river water to make a

172   solution of 15 mg/L. For all experiments, solutions were then added to the quartz flask for

173   experimental irradiation in the Rayonet. Samples were irradiated in a dark room with eight 35 W

174   low-pressure mercury lamps that emitted light centered at 310 nm. The 310 nm lamps have a

175   spectral distribution with a full width at half max of 40 nm; the spectral irradiance of the lamps is

176   shown in Figure S-21. The lamps were uniformly distributed around the vessel, and each sample

177   was irradiated for at least 60 minutes. One set of experiments was conducted in the manner

178   described above, but leaving the lights of the Rayonet turned off; this served as the 'dark control'

179   to ensure any observed degradation was due to the UV-light. In addition, one set of experiments

180   was conducted in the Rayonet with UVC lamps (254 nm) to examine the impact of wavelength.

181

182   An outdoor photolysis experiment was conducted in St. Peter, MN on the Gustavus Adolphus

183   College campus (44° 20' 0" N, 93° 58' 0" W) on June 12-13, 2019, from 11:10 am – 5:10 pm

184   each day (samples were stored in a refrigerator overnight at 9 °C between the two days). The

185   average temperature of a control sample (Milli-Q water) during the experimental time period was

186   31 ± 4 °C. 15 mL samples were placed into 14 quartz test tubes in a 4×6 in. black Rubbermaid

187   notecard box at an upward angle of 45° with the open ends facing east. The irradiated samples

188   were 15 mg/L dicamba in pH 7 phosphate buffer and 6.5×10^{-5} M PNAP/0.198 M pyridine in

189   50:50 Milli-Q water:methanol, the latter as a chemical actinometer. At hour time intervals,

190   duplicate aliquots of 100 µL were removed and placed into amber HPLC vials. The vials were

191   immediately stored in the refrigerator (at 9 °C) for later HPLC analysis.

192

193   Determination of Dissolved Oxygen Concentration in Aqueous Dicamba Solutions

194   A modified Winkler Titration method was used to determine the dissolved oxygen (DO)

195   concentration in oxygen rich and oxygen poor solutions in 1 mM phosphate buffer, pH ~7.[26] O_2

196   (for oxygen rich solutions) or N_2 (for oxygen poor solutions) was introduced into the solutions

197   via a diffusion stone for 15 minutes before taking 1 mL samples every 10 minutes for 90 minutes

198   (the length of one photodegradation experiment). Winkler titration solutions were made based on

199   the literature.[26,27] Samples were added to a small test tube containing 0.5 mL of hexane. To the

200   sample layer, 5 µL of manganese sulfate solution and 5 µL of alkali-azide-iodide solution were

201   added consecutively and allowed to develop for 3 minutes. Concentrated sulfuric acid was added

202   to the sample layer in 0.1 mL volume. After another 3 minutes, the sample layer was transferred

203   to a new small test tube with 1-2 drops of starch solution (and 5 drops of Milli-Q Water for the

204   oxygen sparged solution). The sample was titrated using a 0.000314 M sodium thiosulfate titrant.

205   Photolysis experiments were conducted as described above with both oxygen sparged and

206   nitrogen sparged 15 ppm dicamba solutions.

207

208   Photolysis of Dicamba on Corn Wax Surface

209   Corn wax trials were conducted to simulate conditions of dicamba applied onto the surface of

210   a corn plant. The following methods were adapted from the work of ter Halle et al.[28] The

211   methods have also been used by others.[29–31] For each set of experiments, approximately 160 corn

212   plants (Anderson Seed Company, St. Peter, MN) were grown in a greenhouse to the trifoliate

213   stage, approximately 9-11 days. All corn leaves of each plant were cut off and soaked for two

214   minutes in 75 mL of dichloromethane. The solution was then filtered with a vacuum filter and

215 approximately 10 mL of solution was deposited onto eight glass petri dishes and allowed to

216 evaporate. Evaporating the solvent off left a layer of plant wax remaining on the surface of the

217 petri dishes. Dicamba solutions of 15 mg/L concentration were applied in 10 mL volumes and

218 left to evaporate the solvent off, leaving a solid layer of dicamba. For the experiments with

219 adjuvant, solutions of MAKON® DA-6 (in concentrations of 1 mg/L, 5 mg/L, 10 mg/L, or 15

220 mg/L) with 15 mg/L dicamba were prepared and added to the petri dishes in the same way as

221 above. According to dicamba field application notes, dicamba should be applied to corn at

222 concentrations less than 0.75 lb/acre;[32] applying 10 mL of a 15 mg/L solution to a 5 mm

223 diameter petri dish gives a 0.68 lb/acre equivalent. Measurement of dicamba recovered from the

224 surface prior to irradiation shows overall losses (e.g., volatilization, lack of recovery, degradation

225 in the dark, etc.) are less than 5%. Corn wax plates with applied dicamba samples were exposed

226 to light (irradiance of 0.40 W m^2 at 340 nm) in a Q-Sun Xe-1 Solar Simulator with a Daylight-Q

227 filter (nominal cut-on of 295 nm) at 42 ºC. Samples were taken at time intervals ranging from

228 12-48 hours by reintroducing 10 mL of Milli-Q water before 1 mL aliquots were taken in

229 duplicate. All dicamba irradiated corn wax samples were analyzed using the same HPLC

230 parameters as the dicamba aqueous solution samples. The same method was also used for

231 dicamba with added adjuvant on corn wax surfaces, Diablo® on corn wax surfaces, and on

232 dicamba on glass surfaces.

233

234 Actinometry/Quantum Yield of Dicamba

235 The quantum yield of dicamba under 310 nm lamps in the Rayonet and under the Xe lamps in

236 the Q-Sun solar simulator and in solutions of varying water quality conditions was determined

237 using p-nitroacetophenone/pyridine as an actinometer. A 6.5×10^{-5} M PNAP/0.198 M pyridine

238 solution was made in 50:50 Milli-Q water:methanol and was irradiated using under 310 nm

239 lamps in the Rayonet RPR-100 photochemical reactor for 90 minutes or in the Q-Sun solar

240 simulator for 32 hours. In the Rayonet, 1 mL aliquots were sampled in duplicate every 5 minutes

241 and placed in amber HPLC vials. In the Q-Sun, 100 µL aliquots were sampled in quadruplicate

242 every 1-2 hours. The samples were then analyzed in the HPLC using the methods described

243 above. The quantum yield of dicamba was calculated from Eq 1 (adapted from Leifer eq 6.18):[33]

244 $$\phi_D = \frac{k_D}{k_{PNAP}}\left\{\frac{\Sigma_\lambda \varepsilon_{\lambda,PNAP}L_\lambda}{\Sigma_\lambda \varepsilon_{\lambda,D}L_\lambda}\right\}\phi_{PNAP} \quad \text{Eq 1}$$

245 where k_D and k_{PNAP} are the first-order reaction rate constants for dicamba and PNAP, $\varepsilon_{\lambda,D}$ and

246 $\varepsilon_{\lambda,PNAP}$ are the molar absorptivity (M^{-1} cm^{-1}) at each wavelength, λ, for dicamba and PNAP, L_λ

247 is the irradiance at wavelength, λ, (einstein cm^{-2} day^{-1}) and ϕ_{PNAP} is the quantum yield for PNAP

248 (ϕ_{PNAP} = 0.0169[Pyridine]). The sums in Eq 1 were summed over wavelengths of 270 – 350 nm

249 for the Rayonet 310 nm lamps and over wavelengths of 280 – 400 nm for the Q-Sun Xe lamps

250 (see Figure S-21 for spectra of the lamps). The daily-average solar irradiance spectrum for June

251 21 at 40° N latitude from Apell and McNeill was used to determine the quantum yield of

252 dicamba in the outdoor experiments.[34]

253

254 Determination of Environmental Half-Lives

255 The environmental half-life of dicamba was calculated using the GCSOLAR model developed

256 by Zepp and Cline.[35] This program transforms the laboratory data collected (UV-Vis spectra of

257 dicamba and water samples and quantum yields) into environmentally relevant half-lives. The

258 following input parameters were used: quantum yield of dicamba in aqueous solution irradiated

259 in the Q-sun solar simulator, molar absorptivity coefficients of dicamba and MN River water,

260 longitude of 94° W, clear sky, typical ozone concentration in the atmosphere, default depth

261 parameters and water refraction index, and sea level. A series of latitudes were used as input:

262 30°, 40°, 50°, 60° N. The half-lives obtained were integrated over the entire day.

263

264 Preparation and Analysis of Dicamba Photoproducts

265 A 40 mg/L solution of dicamba in Milli-Q water was irradiated under 310 nm lamps in the RPR-

266 100 for 70 minutes, collecting samples every five minutes. The higher concentration and the

267 RPR-100 were used for photoproduct analysis for analytical measurement reasons. The

268 photoproduct separation and mass spectrometry was performed for time samples at 0, 35, and 70

269 minutes using an Agilent 1290 Infinity II LC coupled with an Agilent 6545XT AdvanceBio

270 LC/Q-TOF. The mass analyzer was calibrated with a standard tuning compound mixture

271 (Agilent, p/n: G1969-85000). The chromatographic separation was performed with a 50 mm x

272 2.1 mm i.d. Eclipse Plus C18, 1.8b micron, S/N: USDAY 40893 column (Agilent) with a mobile

273 phase consisting of %A 1% formic acid in Milli-Q water, %B acetonitrile and a gradient of 2-40-

274 75-2-2% B from 0.00-3.50-4.00-4.01-5.00 minutes. The flow rate was 0.5 mL/min, 5 μL sample

275 injection volume, 36°C column temperature and 50:50 split between the MS and DAD detector

276   set at 254 and 220 nm wavelengths. Tandem MS was done in negative ion mode with the

277   following electrospray ionization parameters: 4000 V capillary voltage, 2000 V nozzle voltage,

278   325°C gas temperature, 5 L/min drying gas flow, 25 psig nebulizer pressure, 275°C sheath gas

279   temperature, and 12 L/min sheath gas flow. An 80 V fragmentor voltage for both MS dimensions

280   was used and had a 45 V skimmer and OCT 1 FR Vpp at 750 V for the MS TOF. For both

281   dimensions, the m/z range was 50 - 970 m/z with an acquisition rate of 5 spectra/s for dimension

282   1 and 1.5 spectra/s for dimension 2 (1152 and 3948 transients/spectrum

283   respectively). MassHunter™ Qualitative Analysis software package, version B.08.00 (Agilent

284   Technologies) was used to extract mass spectra from the separated photoproducts and to predict

285   putative photoproduct molecular formulas.

286

287   Gaussian 09[36] with WebMO graphical interface, version 17.0.012e, was used to examine the

288   molecular energies of photoproducts, including possible isomers. All data presented are from

289   density functional theory calculations for geometry optimization and frequency calculations

290   using B3LYP functionals with the 6-311+G(2d,p) basis set. The default conditions of 298.15 K

291   and 1.0 atm were used for thermochemistry calculations.

292

293   Rate Constant Data Analysis

294   All reported pseudo-first-order rate constants were obtained from weighted linear least-squares

295   analysis of the experimental data (regressing ln[C] versus time, where C equals the molar

296   dicamba concentration). The weighting factors used for the regression (typically $1/\sigma_Y^2$, where

297   σ_Y^2 is the variance on each value of ln[C]) were set equal to C^2 due to the transformation

298   variable.[37] The use of this weight reduces the effect of the later time points (which are likely to

299   have greater variance and error) on the fit of the regression line, yielding more accurate reaction

300   rate constants. Most aqueous experiments were conducted in at least duplicate, and Table 1 lists

301   the number of trials for each set of experiments, n. The standard deviations for experiments in

302   Table 1 with n ≥ 2 are the standard deviations over the trials, and the standard deviations for

303   experiments with n = 1 is the standard deviation of the regression fit (used as an approximation

304   as a true standard deviation was unable to be calculated).

305

306   RESULTS AND DISCUSSION

307

308   Aqueous Experiments

309   Kinetics of Dicamba Photolysis

310   The UV-Vis spectra of dicamba as a function of irradiation time is shown in Figure 1. As can be

311   seen in the figure, the absorbance peak near 203 nm, corresponding to dicamba, decreases with

312   increasing irradiation time. There is an isosbestic point near 235 nm formed between the

313   decreasing dicamba peak and the increasing peak with a center near 254 nm.

314

315   Each photolysis reaction of dicamba examined showed an exponential decrease of dicamba,

316   suggesting that the photodegradation follows a first order or pseudo first order reaction

317   mechanism. Figure 2 shows a selection of the photolysis data, illustrating the first order nature of

318   the reaction. The figure shows a photolysis experiment (conditions: 15 mg/L dicamba buffered

319   with 1 mM phosphate buffer at pH 7, irradiated with 310 nm light in the Rayonet) and an

320   experiment conducted in the dark (conditions: 15 mg/L dicamba buffered with 1 mM phosphate

321   buffer at pH 7, with no irradiation). The dark control experiment showed no loss of dicamba over

322   70 minutes and confirmed that dicamba was not lost via evaporation in the aqueous solution

323   photoreaction chamber. The photolysis experiments of dicamba, applying 310 nm irradiation to a

324   15 mg/L solution of dicamba buffered to pH 7, in a quartz photoreaction flask (experiment

325   conducted n = 6 times), yielded a photodegradation rate constant of k = 23.0 ± 2.9 day^{-1}. Also

326   illustrated in Figure 2 are the kinetic data plots for two additional experiments: irradiation of

327   dicamba in the Rayonet photoreactor with a) an oxygen desaturated solution and b) with addition

328   of 5 mM H_2O_2. These two reactions will be discussed further below. These four rate constants

329   can be found in Table 1, a summary of all rate constants from this work. The Supporting

330   Information contains all the plots (S1-S19) used to obtain the aqueous rate constants in Table 1.

331

332   Table 1 also provides the rate constants for the experiments completed with aqueous solutions in

333   the Q-Sun solar simulator (k = 1.3 ± 0.7 day^{-1}) and outdoors in June 2019 (k = 0.04 ± 0.03. day^{-1}).

334   These two experiments also had an exponential decrease of dicamba over irradiation time, but

335   the reaction rates are much slower than those for the reactions conducted in the Rayonet. The

336   slower rate is presumably due to the spectra of light from the two light sources: both the Q-Sun

337   solar simulator and the sun have a cut-off at 295 nm which limits exposure to some of the higher

338   energy wavelengths present in the Rayonet. The quantum yield for dicamba at pH 7 irradiated in

339   the Q-Sun was determined to be 0.0013, and the quantum yield for dicamba outdoors was

340   0.0012. These quantum yields, which are calculated relative to photon flux from each light

341   source, are nearly identical, showing that the Q-Sun solar simulator is a good lab based light

342   source to use to examine the environmental fate of dicamba.

343

344   Dicamba photolysis in varied pH and wavelength

345   The impact of wavelength on the photodegradation of dicamba was examined in the Rayonet

346   reactor by using both UVC (254 nm) and UVB (280 – 340 nm, centered at 310 nm) lamps. The

347   observed rate constant for the photodegradation of dicamba under 254 nm light was 56.2 ± 2.9

348   day^{-1} (Figure S2). This rate constant is a factor of 2 larger than the rate constant obtained under

349   the 310 nm lamps, and two orders of magnitude larger than the reaction in the Q-Sun. The

350   difference in degradation observed with the different lamps is due to differences in photon flux

351   and energy of the photons from the two sets of lamps, the differences in absorbance of light by

352   dicamba at the two wavelengths, and possibly due to different reaction mechanisms. Since UVC

353   light is not environmentally relevant, no further work was done at this wavelength. Although the

354   Rayonet UVB light source is not a perfect model for environmental light sources, the Rayonet

355   UVB light was used for a series of further experiments to more deeply explore the

356   photochemistry of dicamba as these experiments could be conducted more quickly than

357   experiments outdoors or in the Q-Sun solar simulator, allowing time for more exploration of the

358   photochemical reactions. In addition, a quick look at the irradiated samples from the Q-Sun on

359   the LC-MS showed similar photoproducts to the samples from the samples irradiated with the

360   Rayonet UVB lamps, suggesting that the mechanisms may be similar.

361

362   The pKa of dicamba has been observed to be about 1.9, and the molecule is primarily

363   deprotonated at a pH of 7.[2] Despite the fact that dicamba will be in the carboxylate form in

364   natural waters, there may be environmental circumstances where the protonated form may be

365   important. Therefore, experiments of dicamba photolysis in aqueous solutions were conducted

366   under UVB light in the Rayonet in HCl solutions at pH 1. A rate constant of 20.2 ± 1.4 day^{-1} was

367   observed, suggesting that the reaction is slightly slower in acidic conditions than in the solutions

368   at pH 7. Although the absorbance of 310 nm light is similar for the solutions buffered at both pH

369   1 and pH 7 (see Figure S-21), the quantum yield of the protonated form of dicamba ($\phi = 0.048$)

370   is lower than that of the deprotonated form ($\phi = 0.073$) which leads to the observed slowing of

371   the reaction under acidic conditions. Thus, the slower reaction at pH 1 is due almost entirely due

372   to the lower quantum yield for the protonated form. The favoring of photodegradation in the

373   anionic form has also been observed for other herbicides with a benzoic acid moiety.[38,39] The

374   quantum yields obtained here can also be compared to that obtained by Aguer et al.; these

375   authors obtained a quantum yield of 0.022 for the deprotonated form of dicamba at a wavelength

376   of 275 nm.[2] Aguer et al. also observed that the absorbance of acidic solutions of dicamba was

377   greater than the absorbance of basic/neutral solutions as is shown from this work in Figure S-21.

378   Although the wavelengths used in the two studies (this one and the one by Aguer et al.) differ

379   slightly, the quantum yields are found to be on the same order of magnitude. However, both the

380   quantum yields from the Rayonet experiment and the Aguer et al. paper are an order of

381   magnitude larger than the quantum yields obtained from the Q-Sun and outdoor experiments due

382   to the wavelengths of light used in each experiment. For environmental purposes, the quantum

383   yield from the Q-Sun and/or outdoor experiment should be used.

384

385   Environmental Direct Photolysis Half-Lives of Dicamba

386   Using the quantum yield of dicamba at pH 7 under the Xe lamp of the Q-Sun solar simulator

387   (i.e., $\phi = 0.0013$), the GCSOLAR model was used to determine the environmental direct

388   photolysis half-lives dependent on the season and the degree of latitude in pure water and in

389   Minnesota River water. These direct photolysis half-lives are presented in Table 2. As seen in the

390   table, the half-lives for dicamba range from 3.74 to 97.7 days under these conditions. As

391   expected, half-lives are longer in the winter months and at higher latitudes. Overall, this analysis

392   suggests that dicamba will photodegrade in the environment within days in the typical growing

393   season (summer) and crop locations (latitudes 35º – 45º N) in the United States. These half-lives

394   are on the same order of magnitude as those reported for degradation in aerobic soil in the EPA

395   registration for dicamba.[40]

396

397   Dicamba photolysis in varied oxygen concentration

398   Photodegradation experiments were conducted in oxygen sparged and nitrogen sparged solutions

399   under UVB light in the Rayonet to further examine the role of oxygen in the photodegradation of

400   dicamba. The average dissolved oxygen content in the oxygen sparged solution was 13 ± 4 mg/L

401   with no significant drop in dissolved oxygen content over the 90 minutes. The average dissolved

402   oxygen content in the nitrogen sparged solution was 2.8 ± 0.8 mg/L with no significant change in

403   dissolved oxygen content over the 90 minutes; this corresponds to approximately 1/5th of the

404   dissolved oxygen in the oxygen sparged solution. It was assumed that the addition of 15 mg/L of

405   dicamba would not alter the dissolved oxygen concentration in the buffered solutions, and

406   Winkler titrations were not repeated with dicamba containing aqueous solutions prior to the

407   photolysis.

408

409   The photodegradation rate constant in the nitrogen sparged solution was determined to be $58 \pm$

410   29 day^{-1}, a factor of three greater than that of the photodegradation rate constant in the oxygen

411   sparged experiment (21.6 ± 4.3 day^{-1}). The kinetic data from the nitrogen sparged solution can be

412   seen in Figure 2. The inhibiting effect of oxygen has also been observed in the photolysis of 5-

413   halogenosalicylic acids,[41] compounds with structural similarities to dicamba, and in the

414   photolysis of chlorothalonil[42]. Using laser flash photolysis and computational chemistry

415   calculations, the authors of the paper on halogenosalicylic acids were able to show that oxygen

416   quenched the triplet excited state of the acids.[41] Given the structural similarities of dicamba to

417   these acids, it is hypothesized that the triplet excited state of dicamba is important in its

418   photochemistry and that oxygen acts as a quencher of this state. At reduced oxygen levels, the

419   lifetime of the triplet is longer, leading to faster photoreactions.

420

421   Diablo® and adjuvants

422   The rate constant of Diablo® photodegradation in aqueous solution under UVB light in the

423   Rayonet, 21.6 ± 1.4 day^{-1}, was statistically consistent with the rates seen with aqueous solution

424   experiments of dicamba (Table 1). This is not necessarily intuitive as the additional ingredients

425   in the commercial mix could interact with the dicamba and/or the light to lead to a different

426   reaction rate and/or mechanism.

427

428   As discussed in the introduction, one category of molecules added to commercial herbicides

429   mixtures are adjuvants, designed to help the solutions spread on surfaces. A series of

430   experiments were conducted to explore the impact of these adjuvants on the photodegradation of

431 dicamba. The concentrations and types of adjuvants used in commercial forms of dicamba are

432 proprietary, but there are several surfactants available on the market. Here, a solution of 5 mg/L

433 MAKON® DA-6, an isodecyl alcohol ethoxylate, and 15 mg/L dicamba was tested to model a

434 commercial formulation in solution. The rate constant for the model commercial formulation,

435 33.1 ± 7.2 day^{-1}, was significantly higher than the aqueous solution experiments of dicamba.

436

437 Several papers in the literature have found that nonionic surfactant molecules can photosensitize

438 organic molecules such as herbicides.[43–50] The photosensitization of the dicamba photolysis in

439 the solutions with DA-6 could be due to micelle formation changing the environment in solution,

440 from energy transfer between the herbicide and surfactant, and/or indirect photolysis from the

441 formation of other reactive species. Micelles can form in solutions with surfactant if the

442 concentration of surfactant is above the critical micelle concentration (cmc). For Makon DA-6,

443 an isodecyl alcohol ethoxylate with 6 ethoxylate units, the cmc is estimated to be above 400

444 ppm.[51] For the experiments presented here, with 5 ppm DA-6, no micelles should be formed.

445 Experiments verifying this conclusion are described in the Supporting Information. Micelles,

446 therefore, should not be the reason for the enhanced photodegradation. No experiments were

447 conducted to test the hypothesis that energy transfer may be leading to the photosensitization, but

448 this has been observed in the literature on photochemistry and nonionic surfactants.[45–48]

449

450 To investigate whether the adjuvant was contributing to an indirect photolysis pathway,

451 quenchers for singlet oxygen (5 mM l-histidine) and hydroxyl radical (1% isopropanol) were

452 separately added to solutions of adjuvant/dicamba and irradiated. The rate constants for the

453 indirect photolysis experiments of 15 mg/L dicamba with 5 mg/L DA-6 using l-histidine and

454 isopropanol as quenchers were 20.2 ± 2.9 day^{-1} and 24.5 ± 5.8 day^{-1} respectively (Table 1).

455 These photodegradation rate constants are consistent with the direct photodegradation rate

456 constant of dicamba, suggesting that there may be indirect photolysis occurring in these

457 solutions. It remains unclear what reactive species may be forming in these reactions, and how

458 they are formed, but it is known that dicamba will react with hydroxyl radicals (the literature

459 gives rate constant for the reaction of dicamba with hydroxyl radical as either $k_{OH} = 1.3 \times 10^9$

460 $M^{-1}s^{-1}$ or 3.5×10^9 $M^{-1}s^{-1}$ at pH 7 and T = 20 °C).[52,53] We also conducted an experiment examining

461 the susceptibility of dicamba to hydroxyl radical reactions by irradiating a 15 mg/L dicamba

462   solution spiked with 5 mM H_2O_2. When irradiated at 310 nm, H_2O_2 can produce hydroxyl

463   radicals (quantum yield for this reaction at 308 nm is 1.93±0.39).[54] As can be seen in Table 1 and

464   in Figure 2, the photodegradation rate constant for dicamba in the H_2O_2 spiked experiment was

465   93.6 ± 2.9 day^{-1}, indicating that dicamba photodegradation rates are much faster in the presence

466   of hydroxyl radicals. Although the H_2O_2 experiment illustrates that dicamba can react with

467   hydroxyl radicals, it does not provide evidence that hydroxyl radicals are involved in the

468   experiments with the surfactant DA-6. Overall, it has proven challenging to conclude exactly

469   why the surfactant experiments show an increase in photodegradation rate.

470

471   Dicamba photolysis in varied natural organic matter (NOM) concentration

472   Natural organic matter (NOM) is found in all river waters, commonly at concentrations between

473   1 and 10 mg/L.[55] The structure and chemical composition of NOM varies due to soil type,

474   location, biological degradation, and other factors. In these experiments, Suwannee River NOM,

475   ordered from the International Humic Substances Society, was used as a model NOM. This

476   NOM largely consists of C (52.47% by mass), O (42.69% by mass), H (4.19% by mass), and N

477   (1.10% by mass) and should be negatively charged at pH values of 6-9 due to carboxylic acid

478   functional groups. It has been shown by previous groups that the presence of NOM in water

479   samples can either increase[56–58] or decrease[38,58–62] photodegradation rates. The increase in

480   reaction rates is attributed to the ability of NOM to produce reactive oxygen species such as

481   hydroxyl radicals and/or triplet NOM, and the decrease in rates is typically attributed to

482   screening of light by the NOM.

483

484   As can be observed in Table 3, and Figure S-16, an inverse relationship between NOM

485   concentrations and degradation rates of dicamba was observed in NOM/dicamba experiments.

486   The addition of 1.2 mg/L NOM to 15 mg/L of dicamba caused no change in reaction (k = 23.0 ±

487   1.4 day^{-1}); adding 5.2 mg/L of NOM to 15 mg/L dicamba slowed the reaction down and yielded

488   rate constant of 15.8 ± 1.4 day^{-1}; and adding 10.0 mg/L of NOM to 15 mg/L dicamba yielded a

489   rate constant of 13.0 ± 1.4 day^{-1}. These reaction rate constants suggest that there is no

490   measurable photosensitization, but it may be likely that light screening is occurring. To test for

491   the latter, the screening models presented in Leifer's "The Kinetics of Environmental Aquatic

492   Photochemistry: Theory and Practice" book and in Schwarzenbach, Gschwend, and Imboden's

493   Environmental Organic Chemistry book, were used to correct the measured rate constants for

494   screening:

$$S(\lambda) = \frac{1 - 10^{-D(\lambda)\alpha(\lambda)z_{mix}}}{2.3z_{mix}D(\lambda)\alpha(\lambda)} \quad \text{Eq 2}$$

495

496   where $S(\lambda)$ is the screening factor, $D(\lambda)$ is the distribution function (equal to 1 in these

497   experiments), z_{mix} is the vertical distance in a mixed body of water (equal to 4.6 cm in these

498   experiments), and $\alpha(\lambda)$ is the attenuation coefficient of the medium.[33,58] $\alpha(\lambda)$ was obtained from

499   UV-Vis spectra of NOM and dicamba solutions, similar to the work of Espy, et. al.[38] Because the

500   lamps used in the Rayonet photoreactor have a narrow wavelength range, the photodegradation

501   rate constants obtained in the presence of NOM can be corrected for light screening by dividing

502   the rate constants by the screening factor:

$$k_{corr} \approx \frac{k_{obs}^{NOM}}{S(\lambda)} \quad \text{Eq 3}$$

503

504   where k_{obs}^{NOM} is the experimental degradation rate constant for dicamba in the presence of NOM

505   and k_{corr} is the photodegradation rate constant corrected for light screening. Using the equations

506   above, the observed rate constants from the NOM experiments were corrected to account for

507   screening. The corrected rate constants are given in Table 3. As can be seen in the table, the

508   corrected rate constants match (within experimental error) the photodegradation rate constant of

509   dicamba in buffered solution. This shows that the observed decrease in photodegradation rate

510   upon the addition of NOM is accounted for by screening effects.

511

512   Since the experiments with Suwannee River NOM suggested that screening may be an important

513   factor in natural water systems, Minnesota River water was collected and used as a matrix for

514   photodegradation experiments in the lab. The Minnesota River water was collected in St. Peter,

515   MN in June 2019 and June 2020, and was filtered using a Millipore filtering system prior to

516   spiking the water with dicamba to a concentration of 15 mg/L. Although the Minnesota River

517   water was not analyzed, the soil in this area of Minnesota is mostly Lester soil, known to be a

518   loamy soil with nearly equal amounts of sand and silt, slightly lower clay amounts, and soil

519   organic matter in the range of 2-5%.[63] The rate constant from these experiments, along with the

520   screening factor, and corrected rate constant are available in Table 3. The rate constants obtained

521   from these experiments show that photodegradation of dicamba in natural waters is slower than

522   any of the photodegradation experiments with Suwannee River NOM. Although there is a slight

523   difference between the samples collected from the two different years, the absorbance of light by

524   the Minnesota River water is much stronger than in any of the experiments with Suwannee River

525   NOM, and the calculated screening factor for the Minnesota River water is 0.580 in 2019 and

526   0.884 in 2020. From the 2019 value, one would predict screening is more prevalent in that

527   Minnesota River sample as compared to the lab experiments with Suwannee River NOM.

528   However, when the rate constant is corrected using the screening factor, the corrected rate

529   constant is still slower than the photodegradation rate constant of dicamba in buffered solution.

530   The same is observed with the 2020 sample. Hence, screening alone does not account for the

531   observed drop in photodegradation rate constant of dicamba in the Minnesota River water.

532

533   Adsorption of dicamba to a component in the Minnesota River water is a possibility to explain

534   the slower reaction rate in the experiments with the Minnesota River water. Several authors have

535   examined the sorption of dicamba to soils.[64,65] Sakaliene et al., found the adsorption coefficient

536   of dicamba to be the lowest for the series of herbicides they examined, with a K_d value ranging

537   from 0.03 - 0.08 L/kg depending on the soil type. These low K_d values suggest that adsorption is

538   not likely to be the reason for the observed slower reaction rate. This is supported by the fact that

539   dicamba and the NOM are both negatively charged at the pH levels in these experiments, and it

540   has been shown that negatively charged organic species will adsorb more weakly than the related

541   neutral compound to anionic NOM.[58] In addition, areas of the HPLC peaks from the non-

542   irradiated wax samples align with the non-applied solutions, suggesting no adsorption occurs

543   upon application. Thus, it remains unclear what is causing the reduced photodegradation rate

544   constant of dicamba in the Minnesota River water experiments.

545

546   Photolysis on Epicuticular Corn Wax

547   Recent studies suggest that the matrix environment in which photolysis studies are conducted

548   can affect both photochemical transformation rates and the photoproduct composition.[66–70] For

549   example, the epicuticular wax of most species absorbs light below 350 nm and also contains

550   photosensitizing functional groups such as carboxyl groups.[71–73] Thus, in comparison to

551   photolysis in water samples or other appropriate controls, photolysis of pesticides sorbed to

552   epicuticular wax can be slower (e.g., due to light screening or phase) or faster (e.g., due to

553   photosensitization).

554

555   The experiments with corn waxes are inherently difficult and lengthy due to the time needed to

556   grow the corn, extract and plate the epicuticular wax, and complete the irradiation (so one set of

557   experiments is typically 23-25 days). Dicamba was applied to the surface and irradiated as a

558   solid. Four different sets of corn plants were grown to test the degradation of dicamba on the

559   surface of the waxes. The average rate constant for the photodegradation of dicamba on the

560   surface of corn wax was 0.16 ± 0.01 day^{-1}. The rate constants observed on the corn wax surfaces

561   a factor of ~9 slower than the rate constant from the aqueous solution experiment conducted in

562   the Q-Sun solar simulator, and can be attributed to the solid state of the dicamba during

563   irradiation.

564

565   For comparison, an experiment where dicamba was irradiated after deposition directly on the

566   glass petri dishes was conducted. Other groups interested in the surface photochemistry of

567   herbicides have also used glass or quartz as a comparison.[2,29,30,66,69] The experiments with

568   dicamba directly deposited on the glass petri dishes yielded no statistically significant reaction.

569   This result can be compared to that of Aguer et al. who found that the photolysis rate constant of

570   dicamba was greater when deposited on clay surfaces compared to the photolysis rate when

571   dicamba was deposited on glass.[2] In contrast, the herbicides isoproturon and 2,4-D (and related

572   chlorinated phenoxyacetic acids herbicides) and the plant activator acibenzolar S-methyl were

573   found to react faster on glass surfaces than on paraffin wax.[29,30,66,69] The corn wax used here

574   may have a surface more similar to the clay surfaces used by Aguer compared to paraffin wax

575   surfaces. On the corn waxes, there may be better dispersion across the surface as compared to the

576   glass (perhaps in part because dicamba is anionic in the solid state and glass surfaces are

577   negatively charged).[2] In addition, Aguer et al. found that dicamba is in a microcrystalline form

578   when in the solid state.[2] Photolysis in this state is likely slower because less surface is exposed to

579   light and screening can be expected for the central part of the microcrystals. We speculate that

580   the corn wax might allow the dicamba to spread more evenly across the surface.

581

582   Herbicides are generally applied in the field as formulations including the active ingredient and

583   various adjuvants. The most important class of adjuvants is surfactants, used to reduce the

584   surface tension of the spray solution in the field, allowing droplets to spread on the foliage.

585   Today, the most commonly used surfactants used are alkyl ethoxylated surfactants.[74] A series of

586   experiments were conducted to examine the impact adding adjuvant to the epicuticular wax

587   surfaces has on the photodegradation of dicamba. A surfactant, MAKON® DA-6 (Stepan

588   Company) was added to the surface at several concentrations: 1 mg/L, 5 mg/L, 10 mg/L and 15

589   mg/L (yielding surface concentrations of 5.1×10^{-4} mg/cm^2, 2.6×10^{-3} mg/cm^2, 5.1×10^{-3}

590   mg/cm^2, and 7.7×10^{-3} mg/cm^2 respectively). Table 1 shows the rate constants from these

591   experiments alongside the rate constant from the experiment without adjuvant. Adding adjuvant

592   to the experiment increased the photodegradation rate constant; with 1 mg/L DA-6, the rate

593   constant increased to 0.26 ± 0.03 day^{-1} and with 5 mg/L DA-6, the rate constant increased to 0.32

594   ± 0.03 day^{-1}. This increase is likely due to the adjuvant breaking apart pesticide aggregates as

595   observed by other authors.[69] However, at higher concentrations of DA-6, the rate constant drops

596   again. We believe this is due to experimental limitations; at concentrations of DA-6 above 5

597   mg/L, the corn wax layer starts to physically degrade (visibly detaching from the petri dish and

598   breaking apart), and some dicamba and DA-6 may be present underneath the wax layer rather

599   than at the surface. The corn wax layer also degraded with 15 mg/L DA-6, but the rate constant

600   appears higher than the experiment with 10 mg/L DA-6; since the degradation of the wax was

601   not controlled, perhaps more dicamba remained on the surface in the 15 mg/L experiment. Also

602   shown in Table 1 is an experiment where the commercial product Diablo® was applied to the

603   surface of corn wax. As with the adjuvant experiments, an increase in photodegradation was

604   observed, suggesting that there are other ingredients in the commercial products that lead to

605   faster photodegradation on the wax surfaces. Due to the complexity of these experiments, the

606   photoproducts and degradation pathways of the reaction on the surface of the epicuticular waxes

607   has not been examined.

608

609   Photoproduct Analysis

610   Putative photoproducts were determined using LC-MS-MS analysis of dicamba samples

611   irradiated in aqueous solution under UVB light in the Rayonet at times 0, 35, and 70 minutes.

612   The putative photoproduct structures, measured mass, calculated mass, error, and formula are

613   summarized in Table 4. Proposed structures were determined through fragmentation patterns of

614   tandem mass spectra. The chromatogram collected from the LC-MS is shown in Figure S-23 and

615   a summary of the computational work related to photoproducts is presented in Tables S-2 and

616   S-3. These photoproduct assignments would be at Level 3: Tentative Candidates on the

617   Schymanski scale.[75]

618

619   The structure of Photoproduct A was tentatively assigned through the 2D MS fragmentation

620   pattern of the peak ion 204.9461 m/z with 162.9534 m/z and 124.9797 m/z peak fragments

621   indicating loss of a carboxylic acid group and a chlorine atom respectively (Figure 4).

622   Photoproduct A has a 0.09 ppm error calculated for the measured mass, calculated mass, and

623   chemical formula. The 1D MS chlorine splitting pattern and a calculated 5 double bond

624   equivalence confirmed continued presence of the aromatic ring and carboxylic acid as well as

625   both chlorine atoms. This putative photoproduct shows a loss of a methoxy group and gain of an

626   alcohol group. There is no direct evidence of where the alcohol group adds to the ring, but DFT

627   calculations using B3LYP/6-311+G(2d,p) show that the isomer with the alcohol group meta to

628   the carboxylic acid is 2.20 kcal/mol lower in energy than the isomer with the alcohol group para

629   to the carboxylic acid, and 6.96 kcal/mol lower in energy than the isomer with the alcohol group

630   ortho carboxylic acid. This product has also been observed in work examining the

631   photochemistry of dicamba in the presence of TiO_2.[4,23]

632

633   The structure of Photoproduct B was tentatively assigned using the 1D MS Cl splitting pattern, 5

634   double bond equivalence and the evidence of dimerization within the MS after ESI ionization, all

635   suggesting that the carboxylic acid remained on the ring. The -0.73 error of the measured mass

636   compared to the calculated mass and molecular formula is strong evidence that photoproduct B is

637   an addition of an alcohol group in replacement of a chlorine atom, and replacement of the methyl

638   ether group with an alcohol group. Time dependent DFT calculations using B3LYP/6-

639   311+G(2d,p) showed that the chlorine-carbon bond meta to the carboxylic acid had a larger

640   change in bond length upon excitation. DFT calculations were also used to determine the

641   molecular energy of three possible isomers of this putative photoproduct (differing by where on

642   the ring the two alcohol groups are attached). Two of these isomers are shown in Table 4; isomer

643   B1, with the two alcohol groups ortho to the carboxylic acid, had the lowest energy of the three

644   isomers examined, and is 1.17 kcal/mol lower in energy than photoproduct B2. This

645   photoproduct has also been observed by Fabbri et al. in their work with TiO_2 induce

646 photochemistry of dicamba; these authors also show the product in the form of photoproduct

647 B1.[4]

648

649 The structure of Photoproduct C was tentatively assigned using the 2D MS fragmentation pattern

650 of peak ions 234.9564 m/z and 190.9668 m/z. The 5 double bond equivalence suggests that the

651 carboxylic acid group remains in addition to the ring, and the isomer pattern shows that both

652 chlorines are still attached. Figure 5a shows the 2D MS fragmentation pattern of the 234.9564

653 m/z parent peak ion which indicates the presence of a carboxylic acid group from the 175.94 m/z

654 peak, and two chlorine atoms from the isomer pattern seen in all fragments. The alcohol and

655 ether group were determined from the 175.94 m/z and 139.97 m/z fragments (Figure 5a and 5b).

656 The 2D MS fragmentation pattern of the 190.9668 m/z peak ion confirmed the two chlorine

657 atoms from the isomer pattern visible in all fragments, the loss of an ether group from the 175.94

658 m/z peak, and the loss of an alcohol group from the 139.97 m/z peak (Figure 5b). DFT

659 calculations were again used to determine the energetic stability of possible isomers of this

660 photoproduct. Isomer C1, with the alcohol group para to the carboxylic acid was found to be

661 0.21 kcal/mol lower in energy than isomer C2.

662

663 The structure of Photoproduct D was tentatively assigned through use of the fragmentation

664 pattern of the 1D MS with fragment 157.0064 m/z signaling the loss of the carboxylic acid. The

665 2D MS of the 200.9958 m/z peak ion showed a fragmentation pattern of the loss of the methyl

666 group from the methyl ether and a subsequent loss of the chlorine from peaks 141.9824 m/z and

667 107.0078 m/z subsequently. Thus, we can conclude that the photoproduct contains one chlorine

668 atom, a carboxylic acid group, and a methoxy group. The 5 double bond equivalence and the

669 evidence of dimerization within the MS also show that the carboxylic acid remains on this

670 photoproduct. Time dependent DFT calculations using B3LYP/6-311+G(2d,p) were also

671 completed with photoproduct D, and again the chlorine-carbon bond meta to the carboxylic acid

672 had a larger change in bond length upon excitation. DFT calculations also show that isomer D2

673 is 1.25 kcal/mol lower in energy than D1. Both pieces of computational evidence support that the

674 chlorine meta to the carboxylic acid is the chlorine that has been lost during the formation of this

675 photoproduct. This product has been observed in work examining the photochemistry of dicamba

676   in the presence of TiO_2 but both papers do not assign a location for the alcohol group and

677   chlorine atom.[4,23]

678

679   The structure of Photoproduct E was tentatively assigned using 2D MS of the peak ion 232.9865

680   m/z and the fragmentation pattern suggesting the loss of the carboxylic acid (173.9715 m/z), the

681   loss of a chlorine atom and methyl group (137.9960 m/z), and the loss of an oxygen (125.0238

682   m/z). Fabbri et al. also observed this photoproduct in their work with the photodegradation of

683   dicamba in the presence of TiO_2.[4]

684

685   The structure of Photoproduct F was tentatively assigned from 1D MS by the lack of a chlorine

686   splitting pattern, and the 153.0194 m/z fragment that specified the loss of a carboxylic acid

687   group. The presence of the carboxylic acid group was confirmed by the calculated 5 double bond

688   equivalence. We draw the putative photoproduct with the two alcohol groups taking the place of

689   the missing two chlorine atoms. This is another photoproduct also observed in the work of Fabbri

690   et al.[4] and it has also been observed by Aguer et al.[2] Both of the photoproducts observed in the

691   irradiation of dicamba in aqueous solution in the Aguer paper had a double substitution of

692   chlorine for two alcohol groups; perhaps the singly substituted photoproducts were not observed

693   due to the experimental conditions/irradiation time.[2]

694

695   Figure 6 shows a proposed transformation pathway for the photodegradation of dicamba in

696   aqueous solution. This proposed transformation pathway is similar to that presented by Fabbri et

697   al. for the photolytic degradation of dicamba in UV-TiO_2 and UV-H_2O_2 processes,[4] and is

698   supported by our LC-MS-MS data and putative photoproduct assignments. In the transformation

699   pathway, the first photoproduct formed is photoproduct C, the addition of an alcohol group to

700   dicamba. As with Fabbri,[4] we posit two different photoproducts forming from photoproduct C –

701   photoproduct A, which is a loss of the methoxy group from dicamba, and photoproduct D, loss

702   of one chlorine and the addition of an alcohol group at the position meta to the carboxylic acid.

703   This isomer of photoproduct D is illustrated as it was found to have the lowest energy in the DFT

704   calculations. From photoproduct D, photoproducts B, E, and F form. These photoproducts

705   illustrate further loss of chlorine and addition of alcohol groups to the ring. Photoproduct B also

706   has a loss of the methoxy group on dicamba. Unlike Fabbri et al., we see no further

707 photoproducts/steps in the proposed transformation pathway. We also saw no evidence for the

708 oxidation of the methoxy group Fabbri et al. included in their scheme.[4] We may not be

709 observing these photoproducts due to the different experimental conditions, analytical

710 capabilities, and/or the reaction times that were examined.

711

712 CONCLUSION

713 This project provides details on the environmental fate of dicamba, showing that while the

714 molecule is stable in water and does not undergo hydrolysis, it is susceptible to photolysis when

715 in aqueous solution, on epicuticular waxes, in the presence of surfactants, and in formulation.

716 The quantum yield of dicamba, along with the GCSOLAR program, shows that the

717 environmental half-life of the compound is on the order of days, especially in the spring and

718 summer months in which dicamba is applied to fields. The addition of adjuvants causes an

719 increase in photodegradation of dicamba both in aqueous solution and on epicuticular waxes of

720 corn. Experiments saturating the solutions with nitrogen gas show that the presence of oxygen

721 quenches the photodegradation, suggesting that the triplet excited state of dicamba is involved in

722 the photochemistry. Analysis of photoproducts showed an evolution of aromatic compounds.

723

730

731 AUTHOR CONTRIBUTIONS

732 **Kaitlyn Gruber:** Data Curation, Formal Analysis, Methodology, Validation, Investigation,

733 Visualization, Supervision, Writing – Original Draft, Writing – Review & Editing; **Brittany**

734 **Courteau**: Formal Analysis, Methodology, Validation, Investigation, Visualization, Writing –

735 Original Draft, Writing – Review & Editing; **Maheemah Bokhoree**: Formal Analysis,

736 Validation, Investigation, Visualization, Writing – Original Draft, Writing – Review & Editing;

737 **Elijah McMahon**: Formal Analysis, Investigation, Writing – original draft; **Jenna Kotz**:

738 Formal Analysis, Investigation, Writing – Original Draft; **Amanda Nienow**: Conceptualization,

739 Data Curation, Funding Acquisition, Formal Analysis, Investigation, Methodology, Project

740 Administration, Resources, Supervision, Validation, Visualization, Writing – Original Draft,

741 Writing – Review & Editing

742 SUPPORTING INFORMATION

743 19 first order kinetic plots showing the data used to obtain rate constants, 1 plot showing UV-Vis

744 of dicamba in pH 7 phosphate buffer, in solutions containing NOM, and in MN River water, 1

745 figure showing UV-Vis of dicamba at pH 7 and pH 1 overlaid with the lamp spectra from the

746 Rayonet and Q-Sun photoreactors, a plot showing the critical micelle concentration of MAKON

747 DA-6, a LC-MS chromatogram, and two tables with computational data (geometries and

748 energies).

749 FUNDING SOURCE

752 TABLES

753

754 Table 1: Rate Constants for Dicamba Photodegradation and Number of Trials for Each

755 Experiment, n

Conditions	k / day^{-1}	n
254 nm lamps, pH 7	56.2 ± 2.9	1
No UV-light	No reaction	1
310 nm lamps, pH 7	23.0 ± 2.9	6
310 nm lamps, pH 1	20.2 ± 1.4	2
310 nm lamps, O$_2$ sat'd	21.6 ± 4.3	2
310 nm lamps, N$_2$ sat'd	58 ± 29	2
310 nm lamps, Diablo®	21.6 ± 1.4	3
310 nm lamps, 5 mg/L DA6	33.1 ± 7.2	2
310 nm lamps, 5 mg/L DA6, IPA	24.5 ± 5.8	2
310 nm lamps, 5 mg/L DA6, histidine	20.2 ± 2.9	1
310 nm lamps, 5 mM H$_2$O$_2$	93.6 ± 2.9	1
Outdoors, July 2019, Saint Peter, MN	0.04 ± 0.03	1
Q-Sun Xe lamps, pH 7	1.3 ± 0.7	2
Glass Plate	No reaction	1
Corn Wax	0.16 ± 0.01	1
Corn Wax/Diablo®	0.30 ± 0.03	1
Corn Wax/1mg/L DA-6	0.26 ± 0.03	1
Corn Wax/5 mg/L DA-6	0.32 ± 0.03	1
Corn Wax/10 mg/L DA-6	0.19 ± 0.03	1
Corn Wax/15 mg/L DA-6	0.22 ± 0.01	1

756

757   Table 2: Environmental Direct Photolysis Half-lives of dicamba calculated from GCSOLAR

Season	Latitude (°)	Integrated Half-life (days)	
		DCAM in MN River Water	DCAM in Pure Water
Spring	30	4.23	4.23
	40	4.68	4.68
	50	5.48	5.48
	60	6.83	6.83
Summer	30	3.74	3.74
	40	3.84	3.84
	50	4.08	4.08
	60	4.49	4.49
Fall	30	6.13	6.13
	40	8.21	8.21
	50	12.8	12.8
	60	25.5	25.5
Winter	30	8.63	8.63
	40	14.2	14.2
	50	30.3	30.3
	60	97.7	97.7

758

759
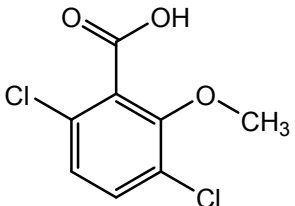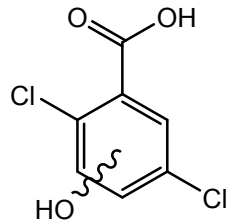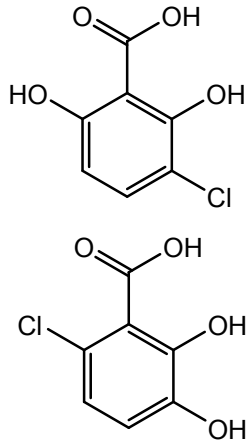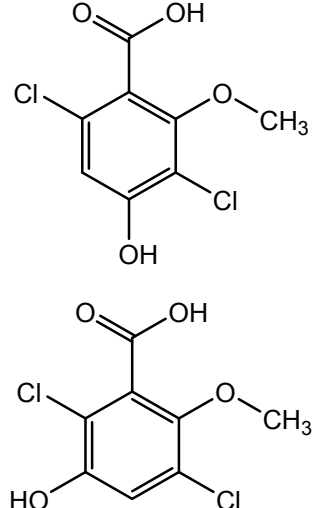
760
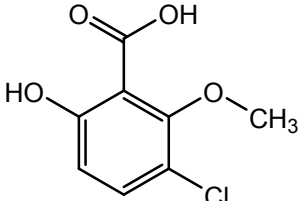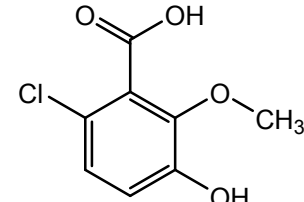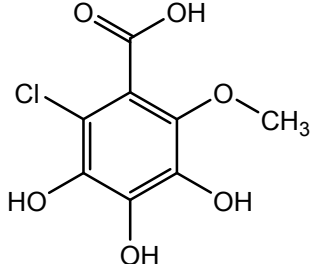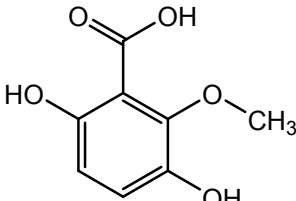
761   Table 3: Experimental (k_{obs}) and Light Screening Corrected (k_{corr}) Rate Constants for Irradiation

762   of pH 7 Dicamba. z_{mix} = 4.6 cm and $D(\lambda)$ = 1 in calculations of $S(\lambda)$.

| Solution	k_{obs} (day^{-1})	$S(\lambda)$	k_{corr} (day^{-1})
Dicamba	23.0 ± 1.4		
Dicamba + 1.2 mg/L NOM	23.0 ± 1.4	0.958	23.0 ± 1.4
Dicamba + 5.2 mg/L NOM	15.8 ± 1.4	0.756	21.6 ± 1.4
Dicamba + 10.0 mg/L NOM	13.0 ± 1.4	0.619	23.0 ± 1.4
Dicamba in MN River water - 2019	8.9 ± 1.4	0.580	15.8 ± 1.4
Dicamba in MN River water - 2020	14.4 ± 1.4	0.884	15.8 ± 1.4

763

764   Table 4: Data from the LC-MS for Each Putative Photoproduct of the Photolysis of Dicamba (40
765   mg/L) Irradiated at 310 nm for 0, 35, and 70 min

Photoproduct	Proposed Putative Photoproduct Structure	Measured Mass ESI [M-H]⁻ m/z	Calculated [M-H]⁻ m/z	Error (ppm)	Formula	DBE	RT / min
Dicamba		218.9629	218.9616	-2.66	$C_8H_6Cl_2O_3$	5	3.227
A		204.9464	204.9459	0.09	$C_7H_4Cl_2O_3$	5	2.915
B B1 – top B2 – bottom		186.9806	186.9798	-0.73	$C_7H_5ClO_4$	5	2.737
C C1 – top C2 – bottom		234.9572	234.9565	-0.7	$C_8H_6Cl_2O_4$	5	2.109

D D1 – top D2 - bottom		200.9964	200.9955	-1.45	$C_8H_7ClO_4$	5	1.919
E		232.9864	232.9853	-2.0	$C_8H_7ClO_6$	5	0.809
F		183.0301	183.0294	-1.05	$C_8H_8O_5$	5	1.795

766

767   FIGURES
768

769
770
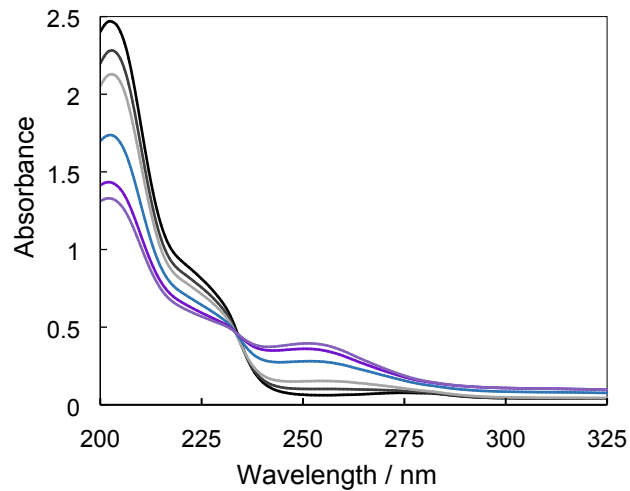
771   Figure 1: A selection of UV-Vis spectra of dicamba irradiated at 310 nm. Looking at 200 nm, the
772   top black line is non-irradiated dicamba and bottom purple line is dicamba irradiated for 55 min.
773   The lines in between were irradiated from 5-50 minutes. The peak at 203 nm corresponds to
774   dicamba; absorbance at that wavelength drops over the irradiation time. Another peak at 254 nm
775   grows in over the irradiation time. An isosbestic point can be seen near 235 nm.

776
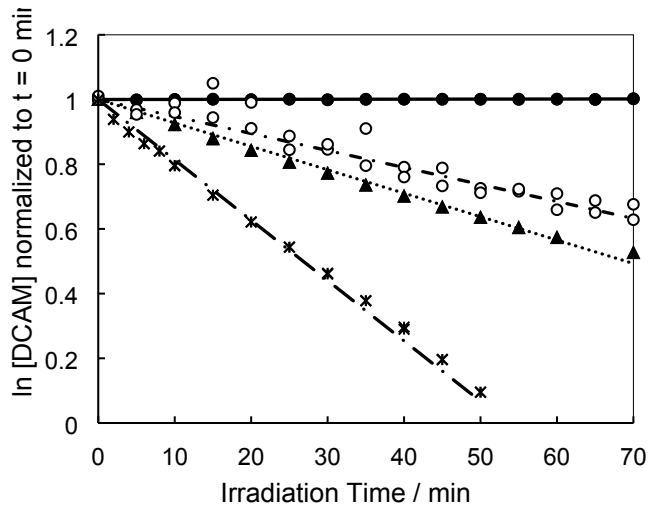
777
778   Figure 2: 15 mg/L at pH 7 dicamba kept the dark (●) and irradiated under 310 nm lamps (▲).
779   Regression lines yield no reaction for the dark control and $k = 23.0 \pm 2.0$ day^{-1} for the irradiated
780   sample. Also shown are 15 mg/L at pH 7 dicamba irradiated under 310 nm lamps in oxygen
781   desaturated solution (◦) and with 5 mM H_2O_2 (∗). Regression lines give $k = 58 \pm 29$ day^{-1} for the
782   experiment with oxygen desaturated solution and 93.6 ± 2.9 day^{-1} for the 5 mM H_2O_2 experiment.
783   These rate constants show the decrease in rate due to the removal of oxygen in the oxygen
784   desaturated solution and the increase in rate due to reaction with hydroxyl radial in the H_2O_2
785   experiment.

786

787
788
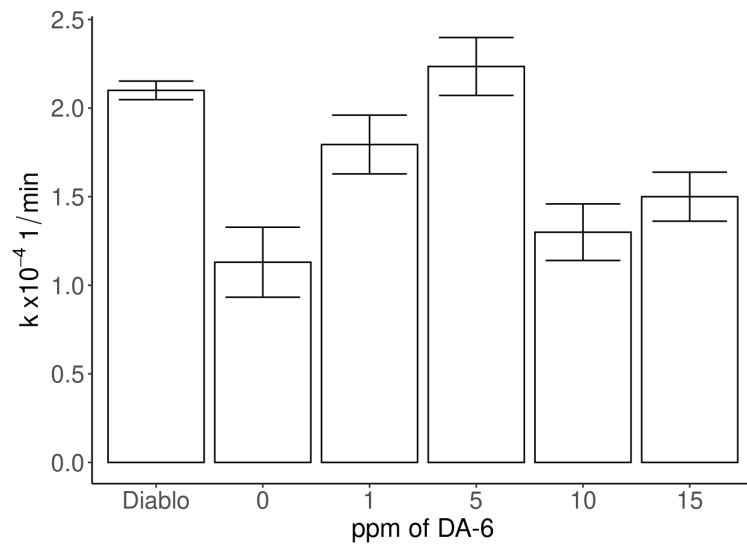
789
790
791 Figure 3: Photodegradation rate constants of dicamba the surfaces of corn wax. Included are:
792 photodegradation rate constant of Diablo®, a commercial product of dicamba, on the surface of
793 corn wax and photodegradation rate constants of dicamba on the surface of corn wax surfaces
794 with 0 ppm adjuvant DA-6, 1 ppm DA-6, 5 ppm DA-6, 10 ppm DA-6, and 15 ppm DA-6.
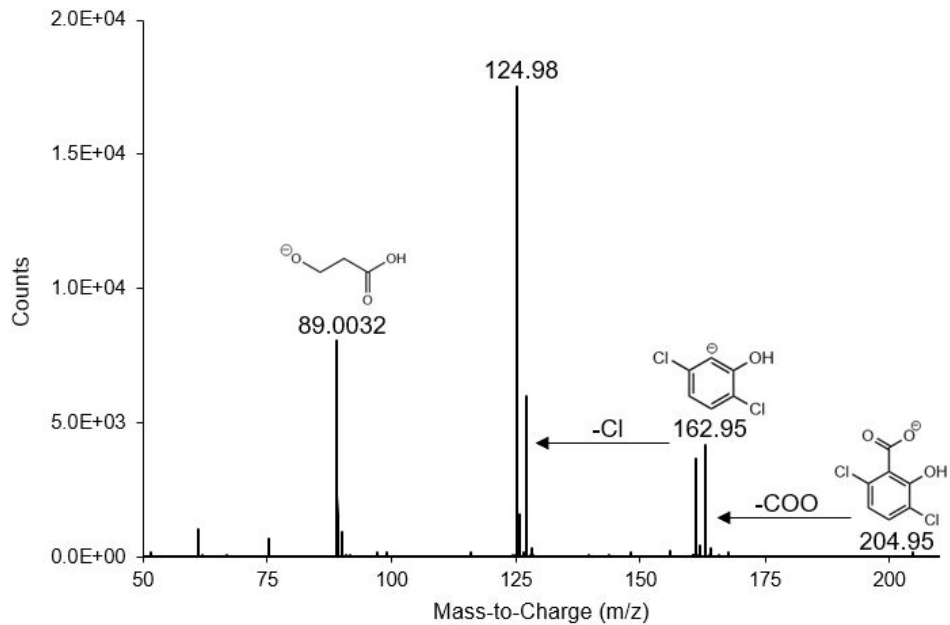
795
796
797   Figure 4. 2D MS of photoproduct A, 204.9461 m/z parent ion peak. The fragmentation pattern of
798   the parent peak ion, 204.9461 m/z, indicates the presence the carboxylic acid group due to the
799   162.95 m/z fragment. The presence of two chlorine atoms was determined from the mass
800   difference and isomer patterns between 124.98 m/z and 162.95 m/z fragments.
801

802
803

804
805

a)

806   b)
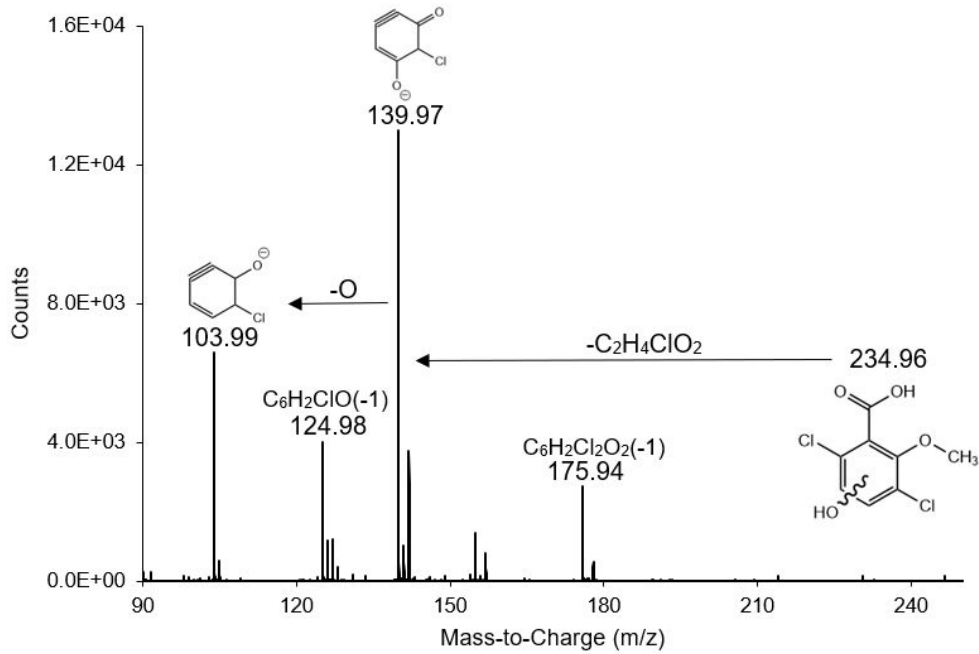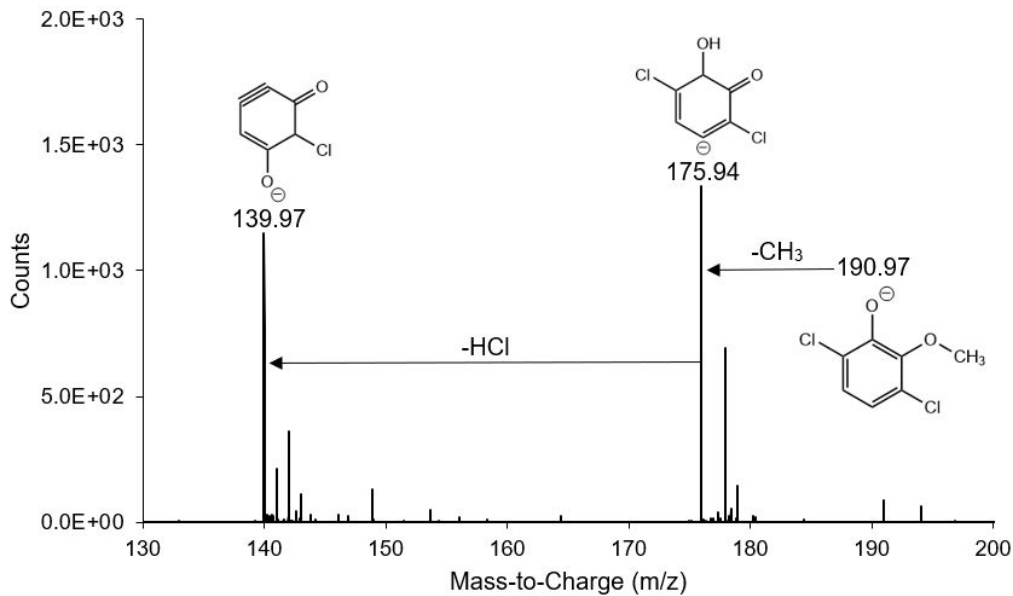
807
808
809 Figure 5. 2D MS of photoproduct C, 234.9564 m/z parent peak ion and 190.9668 m/z base peak
810 ion. a) Fragmentation patterns in the 2D MS of the parent peak ion 234.9564 m/z suggest the
811 presence of a carboxylic acid group, two chlorine atoms, and the ether and alcohol groups meta
812 or para from each other. b) The fragmentation pattern in the 2D MS of the base peak ion
813 190.9668 m/z confirms two chlorine atoms, an ether group from the 175.94 m/z peak, and an
814 alcohol group.
815
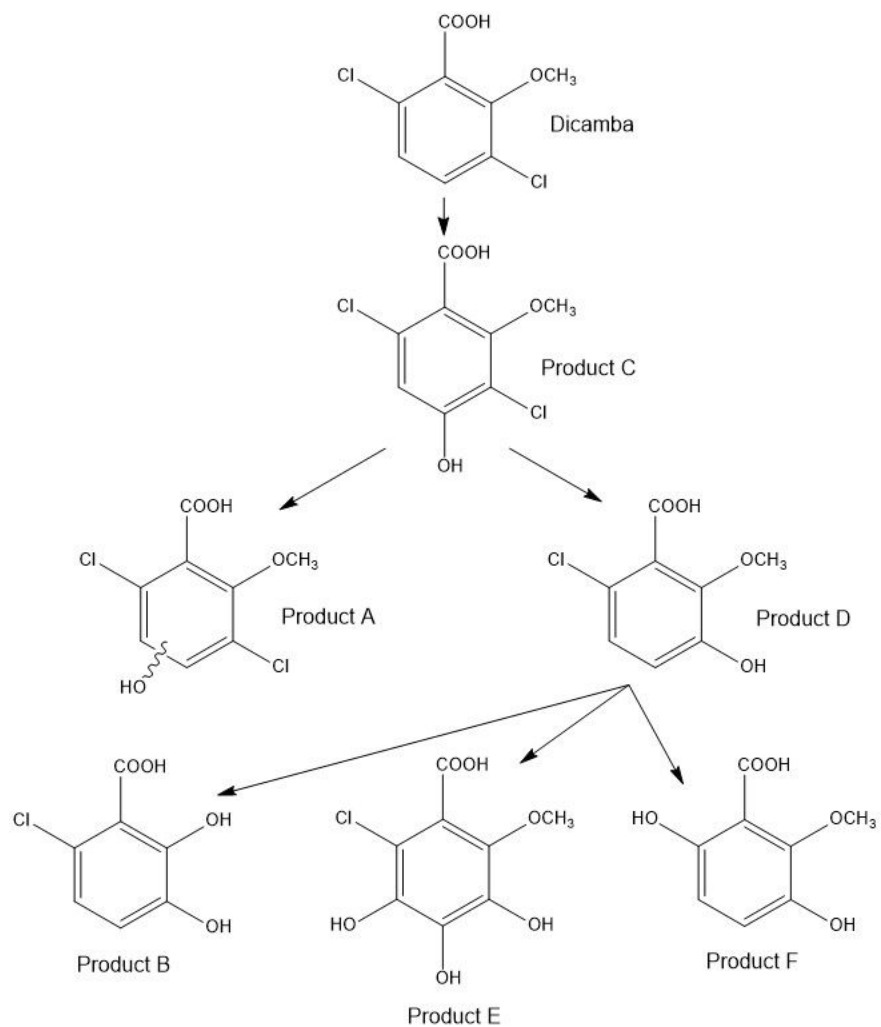
Figure 6. Proposed transformation pathway of photodegradation of dicamba. Proposed transformation pathway was determined from LC-MS-MS data and the similar transformation pathway presented in Fabbri et al.[4] Isomers with the lowest energy as determined by DFT calculations are shown in the proposed transformation pathway.

822   REFERENCES

824   1 Atwood, Donald and Paisley-Jones, Claire, *Pesticides Industry Sales and Usage: 2008-2012*
825   *Market Estimates*, U.S. Environmental Protection Agency.
826   2 J.-P. Aguer, F. Blachère, P. Boule, S. Garaudee and C. Guillard, Photolysis of dicamba (3,6-
827   dichloro-2-methoxybenzoic acid) in aqueous solution and dispersed on solid supports,
828   *International Journal of Photoenergy*, 2000, **2**, 81–86.
829   3 W. Chu and C. C. Wong, The photocatalytic degradation of dicamba in TiO2 suspensions with
830   the help of hydrogen peroxide by different near UV irradiations, *Water Research*, 2004, **38**,
831   1037–1043.
832   4 D. Fabbri, A. B. Prevot and E. Pramauro, Analytical monitoring of the photo-induced
833   degradation of 3,6-dichloro-2-methoxybenzoic acid in homogeneous and heterogeneous
834   systems, *Research on Chemical Intermediates*, 2007, **33**, 393–405.
835   5 Behrens, Richard and Lueschen, W. E., Dicamba Volatility, *Weed Science*, 1979, **27**, 486–493.
836   6 J. F. Egan and D. A. Mortensen, Quantifying vapor drift of dicamba herbicides applied to
837   soybean, *Environmental Toxicology and Chemistry*, 2012, **31**, 1023–1031.
838   7 T. C. Mueller, D. R. Wright and K. M. Remund, Effect of Formulation and Application Time of
839   Day on Detecting Dicamba in the Air under Field Conditions, *Weed Science*, 2013, **61**, 586–
840   593.
841   8 S. D. Strachan, M. S. Casini, K. M. Heldreth, J. A. Scocas, S. J. Nissen, B. Bukun, R. B.
842   Lindenmayer, D. L. Shaner, P. Westra and G. Brunk, Vapor Movement of Synthetic Auxin
843   Herbicides: Aminocyclopyrachlor, Aminocyclopyrachlor-Methyl Ester, Dicamba, and
844   Aminopyralid, *Weed Science*, 2010, **58**, 103–108.
845   9 S. D. Strachan, N. M. Ferry and T. L. Cooper, Vapor Movement of Aminocyclopyrachlor,
846   Aminopyralid, and Dicamba in the Field, *Weed Technology*, 2013, **27**, 143–155.
847   10 Baur, J. R. and Bovey, R. W., Ultraviolet and volatility loss of herbicides, *Archives of
848   Environmental Contamination and Toxicology*, 1974, **2**, 275–288.
849   11 USDA NASS, https://quickstats.nass.usda.gov/, (accessed 17 December 2020).
850   12 Pesticide Use Data System, https://hygeia-analytics.com/tools/puds/by-crop/, (accessed 17
851   December 2020).
852   13 *Roundup Ready 2 Xtend Soybeans: Currently in Phase IV of Monsanto's R&D Pipeline*,
853   Monsanto.
854   14 Erickson, Britt E., *Chemical and Engineering News*, 2016, 94, 15.
855   15 *Roundup Ready 2 Xtend Soybeans Gain EU Import Approval*, Monsanto, St. Louis, MO, 2016.
856   16 H. Hatterman-Valenti, G. Endres, B. Jenks, M. Ostlie, T. Reinhardt, A. Robinson, J. Stenger and
857   R. Zollinger, Defining Glyphosate and Dicamba Drift Injury to Dry Edible Pea, Dry Edible Bean,
858   and Potato, *HortTechnology*, 2017, **27**, 502–509.
859   17 Charles, Dan, *Morning Edition, National Public Radio*, 2020.
860   18 Tong, Scott, *Marketplace, National Public Radio*, 2020.
861   19 A. M. Fogarty and O. H. Tuovinen, Microbiological degradation of the herbicide dicamba,
862   *Journal of Industrial Microbiology*, 1995, **14**, 365–370.
863   20 J. P. Krueger, R. G. Butz and D. J. Cork, Aerobic and anaerobic soil metabolism of dicamba,
864   *Journal of Agricultural and Food Chemistry*, 1991, **39**, 995–999.

865 21 E. W. Pavel, A. R. Lopez, D. F. Berry, E. P. Smith, R. B. Reneau and S. Mostaghimi, Anaerobic
866   degradation of dicamba and metribuzin in riparian wetland soils, *Water Research*, 1999, **33**,
867   87–94.

868 22 P. W. Milligan and M. M. Häggblom, Biodegradation and Biotransformation of Dicamba
869   under Different Reducing Conditions, *Environmental Science & Technology*, 1999, **33**, 1224–
870   1229.

871 23 M. A. Rahman and M. Muneer, Heterogeneous Photocatalytic Degradation of Picloram,
872   Dicamba, and Floumeturon in Aqueous Suspensions of Titanium Dioxide, *Journal of
873   Environmental Science and Health, Part B*, 2005, **40**, 247–267.

874 24 A. Bianco-Prevot, D. Fabbri, E. Pramauro, A. Morales-Rubio and M. de la Guardia, Continuous
875   monitoring of photocatalytic treatments by flow injection. Degradation of dicamba in
876   aqueous TiO2 dispersions, *Chemosphere*, 2001, **44**, 249–255.

877 25 E. Brillas, M. Á. Baños and J. A. Garrido, Mineralization of herbicide 3,6-dichloro-2-
878   methoxybenzoic acid in aqueous medium by anodic oxidation, electro-Fenton and
879   photoelectro-Fenton, *Electrochimica Acta*, 2003, **48**, 1697–1705.

880 26 A. Shriwastav, G. Sudarsan, P. Bose and V. Tare, Modification of Winkler's method for
881   determination of dissolved oxygen concentration in small sample volumes, *Analytical
882   Methods*, 2010, **2**, 1618.

883 27 In *Standard Methods For the Examination of Water and Wastewater*, American Public Health
884   Association, Washington, D.C., 21st Edition., 2005, p. 4:138-4:140.

885 28 A. Ter Halle, D. Drncova and C. Richard, Phototransformation of the herbicide sulcotrione on
886   maize cuticular wax, *Environ Sci Technol Environ Sci Technol*, 2006, **40**, 2989–2995.

887 29 P. P. Choudhury, Leaf cuticle-assisted phototransformation of isoproturon, *Acta Physiologiae
888   Plantarum*, , DOI:10.1007/s11738-017-2471-0.

889 30 P. Choudhury, Leaf-cutin assisted phototransformation of 2,4-D ethyl ester, *Indian Journal of
890   Biochemistry and Biophysics*, 2016, **53**, 227–231.

891 31 S. C. Anderson, A. Christiansen, A. Peterson, L. Beukelman and A. M. Nienow, Statistical
892   analysis of the photodegradation of imazethapyr on the surface of extracted soybean
893   (Glycine max) and corn (Zea mays) epicuticular waxes, *Environ. Sci.: Processes Impacts*, 2016,
894   **18**, 1305–1315.

895 32 *Dicamba Herbicide Application Notes*, Drexel Chemical Company.

896 33 A. Leifer, *The Kinetics of Environmental Aquatic Photochemistry: Theory and Practice*,
897   American Chemical Society, 1988.

898 34 J. N. Apell and K. McNeill, Updated and validated solar irradiance reference spectra for
899   estimating environmental photodegradation rates, *Environmental Science: Processes &
900   Impacts*, 2019, **21**, 427–437.

901 35 R. G. Zepp and D. M. Cline, Rates of direct photolysis in aquatic environment, *Environmental
902   Science & Technology*, 1977, **11**, 359–366.

903 36 M. J. Frisch, G. W. Trucks, H. B. Schlegel, G. E. Scuseria, M. A. Robb, J. R. Cheeseman, G.
904   Scalmani, V. Barone, B. Mennucci, G. A. Petersson, H. Nakatsuji, M. Caricato, X. Li, H. P.
905   Hratchian, A. F. Izmaylov, J. Bloino, G. Zheng, J. L. Sonnenberg, M. Hada, M. Ehara, K. Toyota,
906   R. Fukuda, J. Hasegawa, M. Ishida, T. Nakajima, Y. Honda, O. Kitao, H. Nakai, T. Vreven, J. A.
907   Montgomery, Jr., J. E. Peralta, F. Ogliaro, M. Bearpark, J. J. Heyd, E. Brothers, K. N. Kudin, V.
908   N. Staroverov, R. Kobayashi, J. Normand, K. Raghavachari, A. Rendell, J. C. Burant, S. S.

909 Iyengar, J. Tomasi, M. Cossi, N. Rega, J. M. Millam, M. Klene, J. E. Knox, J. B. Cross, V. Bakken,
910 C. Adamo, J. Jaramillo, R. Gomperts, R. E. Stratmann, O. Yazyev, A. J. Austin, R. Cammi, C.
911 Pomelli, J. W. Ochterski, R. L. Martin, K. Morokuma, V. G. Zakrzewski, G. A. Voth, P. Salvador,
912 J. J. Dannenberg, S. Dapprich, A. D. Daniels, Ö. Farkas, J. B. Foresman, J. V. Ortiz, J. Cioslowski,
913 and D. J. Fox, *Gaussian 09*, Gaussian, Inc., Wallingford, CT, 2009.

914 37 Green, J.R. and Margerison, D., *Statistical Treatment of Experimental Data*, Elsevier Scientific
915 Publishing Company, New York, 1977.

916 38 R. Espy, E. Pelton, A. Opseth, J. Kasprisin and A. M. Nienow, Photodegradation of the
917 Herbicide Imazethapyr in Aqueous Solution: Effects of Wavelength, pH, and Natural Organic
918 Matter (NOM) and Analysis of Photoproducts, *J Agr Food Chem*, 2011, **59**, 7277–7285.

919 39 H. Barkani, C. Catastini, C. Emmelin, M. Sarakha, A. El Azzouzi and J. M. Chovelon, Study of
920 the phototransformation of imazaquin in aqueous solution: a kinetic approach, *J Photoch
921 Photobio A J Photoch Photobio A*, 2005, **170**, 27–35.

922 40 D. Edwards, *Reregistration Eligibility Decision for Dicamba and Associated Salts*, United
923 States Environmental Protection Agency.

924 41 R. Tafer, P. de Sainte-Claire, P. Vicendo, A. Boulkamh and C. Richard, Photochemistry of 5-
925 Halogenosalicylic Acids: Evidence of the Triplet Involvement in the Carbene Formation,
926 *ChemistrySelect*, 2016, **1**, 4704–4712.

927 42 H. He, D. Xiong, F. Han, Z. Xu, B. Huang and X. Pan, Dissolved oxygen inhibits the promotion
928 of chlorothalonil photodegradation mediated by humic acid, *Journal of Photochemistry and
929 Photobiology A: Chemistry*, 2018, **360**, 289–297.

930 43 F. S. Tanaka, R. G. Wien and E. R. Mansager, Effect of nonionic surfactants on the
931 photochemistry of 3-(4-chlorophenyl)-1,1-dimethylurea in aqueous solution, *Journal of
932 Agricultural and Food Chemistry*, 1979, **27**, 774–779.

933 44 F. S. Tanaka, R. G. Wien and E. R. Mansager, Survey for surfactant effects on the
934 photodegradation of herbicides in aqueous media, *Journal of Agricultural and Food
935 Chemistry*, 1981, **29**, 227–230.

936 45 F. S. Tanaka, R. G. Wien and B. L. Hoffer, Photosensitized degradation of a homogeneous
937 nonionic surfactant: hexaethoxylated 2,6,8-trimethyl-4-nonanol, *Journal of Agricultural and
938 Food Chemistry*, 1986, **34**, 547–551.

939 46 Wei. Chu and C. T. Jafvert, Photodechlorination of Polychlorobenzene Congeners in
940 Surfactant Micelle Solutions, *Environmental Science & Technology*, 1994, **28**, 2415–2422.

941 47 F. S. Tanaka, R. G. Wien and R. G. Zaylskie, Photolytic degradation of a homogeneous Triton X
942 nonionic surfactant: nonaethoxylated p-(1,1,3,3-tetramethylbutyl)phenol, *Journal of
943 Agricultural and Food Chemistry*, 1991, **39**, 2046–2052.

944 48 Z. Shi, M. E. Sigman, M. M. Ghosh and R. Dabestani, Photolysis of 2-Chlorophenol Dissolved
945 in Surfactant Solutions, *Environmental Science & Technology*, 1997, **31**, 3581–3587.

946 49 K. Huang, G. Lu, Z. Zheng, R. Wang, T. Tang, X. Tao, R. Cai, Z. Dang, P. Wu and H. Yin,
947 Photodegradation of 2,4,4'-tribrominated diphenyl ether in various surfactant solutions:
948 kinetics, mechanisms and intermediates, *Environmental Science: Processes & Impacts*, 2018,
949 **20**, 806–812.

950 50 X. Li, J. Huang, G. Yu and S. Deng, Photodestruction of BDE-99 in micellar solutions of
951 nonionic surfactants of Brij 35 and Brij 58, *Chemosphere*, 2010, **78**, 752–759.

952 51 P. Mukerjee and K. Mysels, *Critical Micelle Concentrations of Aqueous Surfactant Systems*,
953   Office of Standard Reference Data, National Bureau of Standards, 1971.

954 52 K. L. Armbrust, Pesticide hydroxyl radical rate constants: Measurements and estimates of
955   their importance in aquatic environments, *Environ Toxicol Chem*, 2000, **19**, 2175–2180.

956 53 X. Jin, S. Peldszus and P. M. Huck, Reaction kinetics of selected micropollutants in ozonation
957   and advanced oxidation processes, *Water Research*, 2012, **46**, 6519–6530.

958 54 V. Riffault, T. Gierczak, J. B. Burkholder and A. R. Ravishankara, Quantum yields for OH
959   production in the photodissociation of HNO3 at 248 and 308 nm and H2O2 at 308 and 320
960   nm, *Physical Chemistry Chemical Physics*, 2006, **8**, 1079.

961 55 J. Michalowski, P. Halaburda and A. Kojlo, Determination of humic acid in natural waters by
962   flow injection analysis with chemiluminescence detection, *Analytica Chimica Acta*, 2001,
963   143–148.

964 56 J. J. Werner, K. McNeill and W. A. Arnold, Environmental photodegradation of mefenamic
965   acid, *Chemosphere*, 2005, **58**, 1339–1346.

966 57 S. Halladja, A. Amine-Khodja, A. ter Halle, A. Boulkamh and C. Richard, Photolysis of
967   fluometuron in the presence of natural water constituents, *Chemosphere*, 2007, **69**, 1647–
968   1654.

969 58 R. P. Schwarzenbach, P. M. Gschwend and D. M. Imboden, *Environmental Organic Chemistry*,
970   John Wiley and Sonds, Hoboken, Second Edition., 2003.

971 59 M. Elazzouzi, M. Mekkaoui, S. Zaza, M. El Madani, A. Zrineh and J. M. Chovelon, Abiotic
972   degradation of imazethapyr in aqueous solution, *Journal of Environmental Science and
973   Health, Part B: Pesticides, Food Contaminants, and Agricultural Wastes*, 2002, **B37**, 445–451.

974 60 M. Ramezani, D. P. Oliver, R. S. Kookana, G. Gill and Christopher. Preston, Abiotic
975   degradation (photodegradation and hydrolysis) of imidazolinone herbicides., *J. Environ. Sci.
976   Health, Part B*, 2008, **43**, 105–112.

977 61 A. Latifoglu and M. D. Gurol, The effect of humic acids on nitrobenzene oxidation by
978   ozonation and O-3/UV processes, *Water Res*, 2003, **37**, 1879–1889.

979 62 M. Elazzouzi, A. Bensaoud, A. Bouhaouss, S. Guittonneau, A. Dahchour, P. Meallier and A.
980   Piccolo, Photodegradation of imazapyr in the presence of humic substances, *Fresenius
981   Environmental Bulletin*, 1999, **8**, 478–485.

982 63 *Soil Survey of Nicollet County, Minnesota*, United States Department of Agriculture, Soil
983   Conservation Service, 1994.

984 64 O. Sakaliene, S. K. Papiernik, W. C. Koskinen and K. A. Spokas, Sorption and predicted
985   mobility of herbicides in Baltic soils, *Journal of Environmental Science and Health, Part B:
986   Pesticides, Food Contaminants, and Agricultural Wastes*, 2007, **42**, 641–647.

987 65 Johnson, R.M. and Sims, J.T., Influence of surface and subsoil properties on herbicide
988   sorption by Atlantic Coastal Plain soils, *Soil Science*, **155**, 339–348.

989 66 M. Sleiman, P. de Sainte Claire and C. Richard, Heterogeneous Photochemistry of
990   Agrochemicals at the Leaf Surface: A Case Study of Plant Activator Acibenzolar- *S* -methyl,
991   *Journal of Agricultural and Food Chemistry*, 2017, **65**, 7653–7660.

992 67 A. S. Trivella, S. Monadjemi, D. R. Worrall, I. Kirkpatrick, E. Arzoumanian and Claire. Richard,
993   Perinaphthenone phototransformation in a model of leaf epicuticular waxes., *J. Photochem.
994   Photobiol., B*, 2014, **130**, 93–101.

995   68 S. Monadjemi, A. ter Halle and Claire. Richard, Reactivity of cycloxydim toward singlet oxygen
996   in solution and on wax film., *Chemosphere*, 2012, **89**, 269–273.
997   69 L. Su, J. D. Sivey and N. Dai, Emerging investigator series: sunlight photolysis of 2,4-D
998   herbicides in systems simulating leaf surfaces, *Environmental Science: Processes & Impacts*,
999   2018, **20**, 1123–1135.
1000 70 N. Schippers and W. Schwack, Photochemistry of imidacloprid in model systems, *J. Agric.*
1001   *Food Chem.*, 2008, **56**, 8023–8029.
1002 71 Bianchi, G., Avato, P., and Salamini, F., Surface waxes from grain, leaves, and husks of maize
1003   (Zea mays L.), *Cereal Chemistry*, 1984, **61**, 45–47.
1004 72 K. S. Kim, S. H. Park, D. K. Kim and M. A. Jenks, Influence of Water Deficit on Leaf Cuticular
1005   Waxes of Soybean (*Glycine max* [L.] Merr.), *International Journal of Plant Sciences*, 2007,
1006   **168**, 307–316.
1007 73 P. Cabras, A. Angioni, V. L. Garau, M. Melis, F. M. Pirisi and E. V. Minelli, Effect of epicuticular
1008   waxes of fruits on the photodegradation of fenthion, *J Agr Food Chem J Agr Food Chem*,
1009   1997, **45**, 3681–3683.
1010 74 D. Lavieille, H. A. Ter, P.-O. Bussiere and C. Richard, Effect of a spreading adjuvant on
1011   mesotrione photolysis on wax films, *J Agric Food Chem*, 2009, **57**, 9624–8.
1012 75 E. L. Schymanski, J. Jeon, R. Gulde, K. Fenner, M. Ruff, H. P. Singer and J. Hollender,
1013   Identifying Small Molecules via High Resolution Mass Spectrometry: Communicating
1014   Confidence, *Environ. Sci. Technol.*, 2014, **48**, 2097–2098.
1015